ANALYSIS OF ROLL STABILITY OF THE SPRAYER BASED ON THE EQUIVALENT MECHANICAL MODEL OF LIQUID SLOSHING
/
基于液体晃动等效力学模型的喷雾机侧倾稳定性分析

Jizhou ZHENG[1,2], Yanpeng LI[1], Lan ZHANG[1], Xinyu XUE [3,*] [1]

[1] College of Mechanical and Electronic Engineering, Shandong Agricultural University, Taian, Shandong/ China
[2] Shandong Provincial Key Laboratory of Horticultural Machinery and Equipment, Taian, Shandong / China
[3] Nanjing Institute of Agricultural Mechanization, Ministry of Agriculture and Rural Affairs, Nanjing, Jiangsu/ China
Tel: 02584346243; E-mail: 735178312@qq.com
DOI: https://doi.org/10.35633/inmateh-67-10

Keywords: *sprayer, liquid sloshing, roll stability, dynamic model*

ABSTRACT
In order to analyze the influence of liquid sloshing on the roll stability of the sprayer, the equivalent mechanical model of liquid sloshing was introduced. A multi-degree-of-freedom model of the sprayer chassis was established that includes the effect of liquid sloshing. An E-level road spectrum was constructed based on sinusoid superposition method according to the grade of the field ground unevenness, and the roll stability of the sprayer chassis under these random excitations was investigated. The effects of liquid filling ratio and driving speed were analyzed. The results show that the roll angle decreases with the increase of filling ratio at low speed, but the situation is the opposite at high speed. The vertical acceleration of the vehicle body decreases to some extent under some situations due to the presence of the liquid. In general, both the roll angle and the vertical acceleration increase with the increase of the driving speed, especially in the case of existing liquid sloshing.

摘要
为分析液体晃动对喷雾机侧倾稳定性的影响，引入液体晃动等效力学模型。建立了包含液体晃动影响的喷雾机底盘多自由度动力学模型。根据农田地面不平度等级构建了 E 级路面谱，研究了地面不平激励下喷雾机底盘的侧倾稳定性。分析了充液比和行驶速度的影响。结果表明：侧倾角低速时随液体深度增加而减小，而高速时情况相反。由于液体的存在，车身垂向加速度在某种情形下有所减小。总体来看，侧倾角和垂向加速度都随行驶速度增加而增大，存在液体晃动时更加显著。

INTRODUCTION
The self-propelled boom sprayer has been widely used in the chemical control of crop pests and diseases in farmland due to the advantages of high efficiency and good pesticide application effect. High-clearance or ultra-high-clearance sprayer is usually adopted in order to reduce crop damage, especially for the long-stalked crops such as corn and rice. The engine, cab, water tank and boom are generally placed on the frame in order to reduce the collision with the crop. Thus, high ground clearance means that the center of mass of the sprayer is high, which reduces the roll and pitch stability. Different from other agricultural machinery that is totally made of solid material, the position of the centroid of the sprayer is more sensitive to the attitude because of the fluidity of the fluid in the tank. Unfortunately, there are inevitable obstacles such as bumps and dips on country roads and fields. Furthermore, the large amplitude liquid sloshing produces an impact pressure on the tank wall, and the resulting sloshing force also acts on the sprayer. Obviously, the roll and pitch stability of the sprayer will be affected by this lateral force.

Due to its particularity, researches on high-clearance sprayers mainly focus on local structure design or optimization such as vehicle chassis design (*Chen et al., 2020; Qiu, et al., 2020; Wu et al., 2018; Yang et al., 2014; Zeng et al., 2019*), vehicle or boom attitude control (*Cui et al., 2018; Pochi and Vannucci, 2002; Tahmasebi et al., 2015; Xue et al., 2018; Zhou et al., 2020*), spray monitoring (*Zhai et al., 2018*), etc., while the roll stability is rarely studied (*Ding et al., 2019; Yu et al., 2020*).

[1] *Jizhou Zheng, Prof. Ph.D. Eng.; Yanpeng Li, M.S. Stud. Eng.;Lan Zhang, M.S. Stud. Eng.; Xinyu Xue, Prof. Ph.D. Eng.*.

At present, the research of liquid sloshing on vehicle stability is mainly carried out on road or railway tanks (*Hu et al., 2013*). For transport vehicles on road, rollover accidents mainly come from rapid steering or braking, so the angle of the steering wheel or front wheel is generally used as the input of the system. The road unevenness is often not involved because of the little effect. Different from road transportation vehicles, sprayers face more complex and harsh road conditions despite their relatively low speeds. In addition to the effect of the slowly-changed ramp on the centroid position of the sprayer, rural roads and farmland have not only relatively small but continuous ground unevenness but also large bumps and dips such as ridges and ditches. The liquid in the tank sloshes significantly under these continuous or occasional excitations, and the sloshing force acts on the sprayer, which not only increases the difficulty of manipulation, but also reduces the roll and pitch stability.

In order to investigate the influence on roll stability of liquid sloshing, a mechanical model that is equivalent with the effect of liquid sloshing was introduced. At the same time, the 1/2 car body model that includes the frame, left and right wheel was built to express the roll movement. Then, a coupling model was established by combining these two models. The dynamic response of the system under the excitation of ground unevenness was obtained, and influencing factors of the roll stability were investigated.

MATERIALS AND METHODS

EQUIVALENT MECHANICAL MODEL OF LIQUID SLOSHING

The basic methods of liquid sloshing research can be divided into three categories: theoretical analysis, numerical simulation, and experimental research. The experimental and simulation methods are very useful to observe and explain the liquid sloshing phenomenon, but it is difficult to apply directly in theoretical analysis. In addition, it is not easy to couple the fluid dynamics equation with the vehicle's dynamics model. Therefore, reduced-order models such as pendulum or spring-mass are often used to equate some dynamic characteristics of liquid sloshing in engineering (*Abramson, 1966; Deng et al., 2016; Li et al., 2011; Zheng et al., 2013*). The equivalent mechanical model composed of mass and spring is shown in Fig. 1.

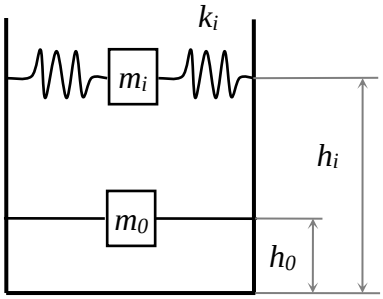

Fig. 1 - Equivalent model of liquid sloshing

The mass, the centroid position, the natural frequency, and the sloshing force and moment of the equivalent system should be equal to the original liquid system. According to this principle, the calculation formula of the physical quantities appeared in Fig. 1 for the rectangular tank is as follows (*Ibrahim, 2005*).

$$m_f = \rho l_f w_f h_f \tag{1}$$

$$m_i = \frac{8}{\pi^3} \frac{\tanh\left(\frac{(2i-1)\pi h_f}{l_f}\right)}{\frac{(2i-1)^3 h_f}{l_f}} m_f \tag{2}$$

$$m_0 = m_f - \sum_{i=1}^{\infty} m_i \tag{3}$$

$$h_i = \frac{h_f}{2} - \frac{\tanh\left(\frac{(2i-1)\pi h_f}{2l_f}\right)}{\frac{(2i-1)\pi}{2l_f}} \tag{4}$$

$$h_0 = \frac{1}{m_0}\sum_{i=1}^{\infty} m_i h_i \tag{5}$$

$$k_i = \frac{8\tanh^2\left(\frac{(2i-1)\pi h_f}{l_f}\right) g}{(2i-1)^2 h_f} m_f \tag{6}$$

where, m_f is the mass of liquid, [kg]; m_i is the i-th motion mass, [kg] and h_i is its position, [m]; m_0 is the fixed mass, [kg] and h_0 is its position, [m]; k_i is the i-th stiffness of the spring, [N/m]; ρ is the density of liquid, [kg/m^3]; g is the gravity acceleration, [m/s^2]; l_f, w_f and h_f are the length, width and height of liquid respectively, [m]; $i = 1, 2, 3\cdots$.

LIQUID SLOSHING – VEHICLE ROLL COUPLING MODEL

The attitude of the sprayer chassis changes due to the uneven ground, and the liquid in the tank fixed on the frame of the chassis also moves. Different from solid, fluid motion not only affects the distribution of the mass but also has an impact pressure on the tank. Thus, more complex dynamics properties will be present for the sprayer than for other agricultural machinery.

The chassis of the self-propelled boom sprayer is mainly composed of frame, engine, suspension, wheels and steering system. The ground roughness excitations directly acting on the wheels are transmitted to the frame through the suspension, causing pitch and roll motions, as shown in Fig. 2. Both of the motions can make the liquid in the tank to slosh, which in turn affects the pitch and roll stability of the sprayer. In this paper, only rolling stability is considered to better understand the nature of liquid sloshing and its effect on the sprayer dynamics.

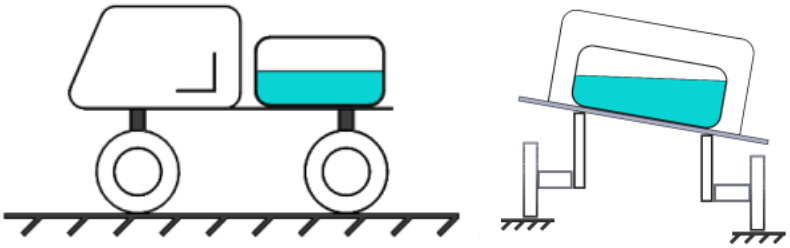

Fig. 2 – Schematic diagram of the sprayer chassis and the tank (left: side view; right: rear view)

The 1/2 car body model is adopted to study the roll stability of sprayers chassis under the conditions of uneven ground. In this model, the vertical movement of the left and right wheel is considered, and the vertical and roll movements of the frame is considered. The roll of the frame causes the liquid sloshing, and the liquid sloshing force in turn affects the roll movement. The coupled dynamics model is shown in Fig. 3.

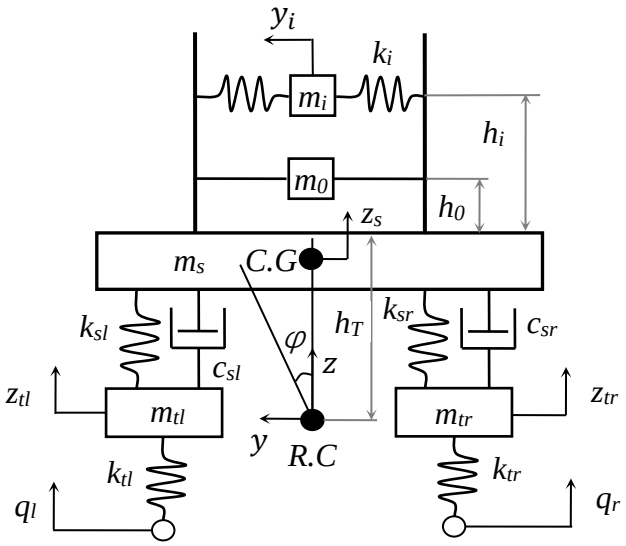

Fig. 3 - Coupling model of the sprayer

The damping of the tire is relatively small, so only its stiffness is considered, and the spring k_t is used to describe its elasticity. The suspension is simulated with the spring k_s and the damper c_s. Assume that the unsprung mass m_t only vibrates in the vertical direction, while the sprung mass m_s moves in a plane around the roll center (R.C).

The Cartesian coordinate system is used to describe the movement of the sprayer. The x-axis is along the longitudinal direction of the vehicle, and its positive direction is the forward direction; the y-axis points to the side of the vehicle, and the left is the positive direction; the z-axis is along the vertical direction, and the positive direction is upward. The dynamic equation of each movement is as follows.

Vertical movement of the frame:

$$\begin{aligned}\left(m_s+m_f\right)\ddot{z}_s=&-\left(k_{sl}+k_{sr}\right)z_s-\left(c_{sl}+c_{sr}\right)\dot{z}_s+\frac{B}{2}\left(k_{sl}-k_{sr}\right)\varphi+\frac{B}{2}\left(c_{sl}-c_{sr}\right)\dot{\varphi}\\&+k_{sl}z_{tl}+c_{sl}\dot{z}_{tl}+k_{sr}z_{tr}+c_{sr}\dot{z}_{tr}\end{aligned} \tag{7}$$

Roll movement of the frame:

$$\begin{aligned}\left(I_{xx}+I_f\right)\ddot{\varphi}=&\frac{B}{2}\left(k_{sl}-k_{sr}\right)z_s+\frac{B}{2}\left(c_{sl}-c_{sr}\right)\dot{z}_s-\frac{B^2}{4}\left(k_{sl}+k_{sr}\right)\varphi-\frac{B^2}{4}\left(c_{sl}+c_{sr}\right)\dot{\varphi}\\&-\frac{B}{2}k_{sl}z_{tl}-\frac{B}{2}c_{sl}\dot{z}_{tl}+\frac{B}{2}k_{sr}z_{tr}+\frac{B}{2}c_{sr}\dot{z}_{tr}-\sum_{i=1}^{\infty}k_i\left[\left(h_T+h_i\right)^2\varphi-\left(h_T+h_i\right)y_i\right]\end{aligned} \tag{8}$$

Vertical movement of wheels:

$$m_{tl}\ddot{z}_{tl}=k_{sl}z_s+c_{sl}\dot{z}_s-\frac{B}{2}k_{sl}\varphi-\frac{B}{2}c_{sl}\dot{\varphi}-\left(k_{tl}+k_{sl}\right)z_{tl}-c_{sl}\dot{z}_{tl}+k_{tl}q_l \tag{9}$$

$$m_{tr}\ddot{z}_{tr}=k_{sr}z_s+c_{sr}\dot{z}_s+\frac{B}{2}k_{sr}\varphi+\frac{B}{2}c_{sr}\dot{\varphi}-\left(k_{tr}+k_{sr}\right)z_{tr}-c_{sr}\dot{z}_{tr}+k_{tr}q_r \tag{10}$$

Where, φ is the roll angle of the sprayer around the x-axis, [°]; z_s is the vertical displacement of the frame, [m]; z_{tl} and z_{tr} are the vertical displacement of the left and right wheel respectively, [m]; y_i is the horizontal displacement of motion mass m_i, [m]; m_s is the mass of the frame (including the tank), [kg]; m_{tl} and m_{tr} are the mass of the left and right wheel respectively, [kg]; I_{xx} is the moment of inertia of the sprung mass around the x axis, [kgm^2]; I_f is the moment of inertia of the liquid in the tank around the x axis, [kgm^2]; k_{sl} and k_{sr} are the stiffness of the left and right suspension respectively, [N/m]; c_{sl} and c_{sr} are the damping coefficients of the left and right suspension respectively, [Ns/m]; k_{tl} and k_{tr} are the stiffness of the left and right tire respectively, [N/m]; h_T is the distance from the bottom of the tank to the roll center, [m]; B is the wheelbase, [m]; q_l and q_r are the input of the left and right wheel respectively, [m].

It can be seen that a roll motion around the x-axis will occur for the frame under the unevenness excitation of the ground, which will cause the liquid in the tank to slosh. The liquid sloshing force acts on the frame via the container wall, which will in turn affect the vehicle's roll movement. So, the motions of frame and liquid are coupled with each other.

It can be calculated from formula (2) that the first-order mass is much larger than the higher-order mass. In other words, the first mode dominates the dynamic response of the system. Therefore, only the first-order mode is taken in the following modeling in order to simplify the calculation. That is, only m_1, h_1, y_1 and k_1 are used.

The state space model of the system can be established by taking y_1, z_s, φ, z_{tl}, z_{tr} and their first-order derivatives as state variables and taking y_1, z_s, φ, z_{tl}, z_{tr} and their second-order derivatives as outputs.

That is, the state vector $x=\begin{bmatrix} y_1 & \dot{y}_1 & z_s & \dot{z}_s & \varphi & \dot{\varphi} & z_{tl} & \dot{z}_{tl} & z_{tr} & \dot{z}_{tr} \end{bmatrix}^{\mathrm{T}}$, and the output vector $y=\begin{bmatrix} y_1 & \ddot{y}_1 & z_s & \ddot{z}_s & \varphi & \ddot{\varphi} & z_{tl} & \ddot{z}_{tl} & z_{tr} & \ddot{z}_{tr} \end{bmatrix}^{\mathrm{T}}$. Where, the superscript T means the transpose of a vector or matrix. The state space model can be written as

$$\begin{aligned} \dot{x} &= Ax + Bu \\ y &= Cx + Du \end{aligned} \tag{11}$$

Where, *A* is the system matrix, *B* is the input matrix, *C* is the output matrix, and *D* is the transfer matrix. $u=\begin{bmatrix} q_l \\ q_r \end{bmatrix}$ is the input vector. The specific expressions of the elements in the matrices *A*, *B*, *C*, and *D* can be derived from the equation (7)-(10), which are listed as follows.

$$A=\begin{bmatrix}
0 & 1 & 0 & 0 & 0 & 0 & 0 & 0 & 0 & 0 \\
-\frac{k_1}{m_1} & 0 & 0 & 0 & \frac{k_1}{m_1}(h_T+h_1) & 0 & 0 & 0 & 0 & 0 \\
0 & 0 & 0 & 1 & 0 & 0 & 0 & 0 & 0 & 0 \\
0 & 0 & -\frac{k_{sl}+k_{sr}}{m_s+m_f} & -\frac{c_{sl}+c_{sr}}{m_s+m_f} & \frac{B(k_{sl}-k_{sr})}{2(m_s+m_f)} & \frac{B(c_{sl}-c_{sr})}{2(m_s+m_f)} & \frac{k_{sl}}{m_s+m_f} & \frac{c_{sl}}{m_s+m_f} & \frac{k_{sr}}{m_s+m_f} & \frac{c_{sr}}{m_s+m_f} \\
0 & 0 & 0 & 0 & 0 & 1 & 0 & 0 & 0 & 0 \\
\frac{k_1(h_T+h_1)}{I_{xx}+I_f} & 0 & \frac{B(k_{sl}-k_{sr})}{2(I_{xx}+I_f)} & \frac{B(c_{sl}-c_{sr})}{2(I_{xx}+I_f)} & -\frac{B^2(k_{sl}+k_{sr})+4k_1(h_T+h_1)^2}{4(I_{xx}+I_f)} & -\frac{B^2(c_{sl}+c_{sr})}{4(I_{xx}+I_f)} & \frac{-Bk_{sl}}{2(I_{xx}+I_f)} & \frac{-Bc_{sl}}{2(I_{xx}+I_f)} & \frac{Bk_{sr}}{2(I_{xx}+I_f)} & \frac{Bc_{sr}}{2(I_{xx}+I_f)} \\
0 & 0 & 0 & 0 & 0 & 0 & 0 & 1 & 0 & 0 \\
0 & 0 & \frac{k_{sl}}{m_{tl}} & \frac{c_{sl}}{m_{tl}} & -\frac{Bk_{sl}}{2m_{tl}} & -\frac{Bc_{sl}}{2m_{tl}} & -\frac{k_{tl}+k_{sl}}{m_{tl}} & -\frac{c_{sl}}{m_{tl}} & 0 & 0 \\
0 & 0 & 0 & 0 & 0 & 0 & 0 & 0 & 0 & 1 \\
0 & 0 & \frac{k_{sr}}{m_{tr}} & \frac{c_{sr}}{m_{tr}} & \frac{Bk_{sr}}{2m_{tr}} & \frac{Bc_{sr}}{2m_{tr}} & 0 & 0 & -\frac{k_{tr}+k_{sr}}{m_{tr}} & -\frac{c_{sr}}{m_{tr}}
\end{bmatrix}$$

$$B=D=\begin{bmatrix}
0 & 0 & 0 & 0 & 0 & 0 & 0 & \frac{k_{tl}}{m_{tl}} & 0 & 0 \\
0 & 0 & 0 & 0 & 0 & 0 & 0 & 0 & 0 & \frac{k_{tr}}{m_{tr}}
\end{bmatrix}^{\mathrm{T}},$$

$$C=\begin{bmatrix}
1 & 0 & 0 & 0 & 0 & 0 & 0 & 0 & 0 & 0 \\
-\frac{k_1}{m_1} & 0 & 0 & 0 & \frac{k_1}{m_1}(h_T+h_1) & 0 & 0 & 0 & 0 & 0 \\
0 & 0 & 1 & 0 & 0 & 0 & 0 & 0 & 0 & 0 \\
0 & 0 & -\frac{k_{sl}+k_{sr}}{m_s+m_f} & -\frac{c_{sl}+c_{sr}}{m_s+m_f} & \frac{B(k_{sl}-k_{sr})}{2(m_s+m_f)} & \frac{B(c_{sl}-c_{sr})}{2(m_s+m_f)} & \frac{k_{sl}}{m_s+m_f} & \frac{c_{sl}}{m_s+m_f} & \frac{k_{sr}}{m_s+m_f} & \frac{c_{sr}}{m_s+m_f} \\
0 & 0 & 0 & 0 & 1 & 0 & 0 & 0 & 0 & 0 \\
\frac{k_1(h_T+h_1)}{I_{xx}+I_f} & 0 & \frac{B(k_{sl}-k_{sr})}{2(I_{xx}+I_f)} & \frac{B(c_{sl}-c_{sr})}{2(I_{xx}+I_f)} & -\frac{B^2(k_{sl}+k_{sr})+4k_1(h_T+h_1)^2}{4(I_{xx}+I_f)} & -\frac{B^2(c_{sl}+c_{sr})}{4(I_{xx}+I_f)} & \frac{-Bk_{sl}}{2(I_{xx}+I_f)} & \frac{-Bc_{sl}}{2(I_{xx}+I_f)} & \frac{Bk_{sr}}{2(I_{xx}+I_f)} & \frac{Bc_{sr}}{2(I_{xx}+I_f)} \\
0 & 0 & 0 & 0 & 0 & 1 & 0 & 0 & 0 & 0 \\
0 & 0 & \frac{k_{sl}}{m_{tl}} & \frac{c_{sl}}{m_{tl}} & -\frac{Bk_{sl}}{2m_{tl}} & -\frac{Bc_{sl}}{2m_{tl}} & -\frac{k_{tl}+k_{sl}}{m_{tl}} & -\frac{c_{sl}}{m_{tl}} & 0 & 0 \\
0 & 0 & 0 & 0 & 0 & 0 & 0 & 0 & 0 & 1 \\
0 & 0 & \frac{k_{sr}}{m_{tr}} & \frac{c_{sr}}{m_{tr}} & \frac{Bk_{sr}}{2m_{tr}} & \frac{Bc_{sr}}{2m_{tr}} & 0 & 0 & -\frac{k_{tr}+k_{sr}}{m_{tr}} & -\frac{c_{sr}}{m_{tr}}
\end{bmatrix}$$

The coupling between the liquid sloshing in the tank and the roll motion of the sprayer chassis under the excitation of ground roughness is the research objective of this paper. In other words, the steady-state response or forced vibration of the coupling system is the focus of our attention. Therefore, the effect of initial conditions is not considered.

The specific values of the elements in each matrix can be obtained from the simulation parameters given in the next section. The uneven ground excitation under the left and right wheels is used as the input, and the response of the system can be obtained by solving the equation (11).

SIMULATION PARAMETERS

Many parameters of the sprayer chassis are predetermined, such as suspension stiffness, damping coefficient, tire type, etc. It is difficult to change them during pesticide application operation, so their effects on roll stability are not considered here. Extracted from a certain type of self-propelled boom sprayer, the parameters used in simulations are listed in Tab.1. It is assumed that the car body is symmetrical about the x-axis to simplify the analysis.

Table 1

Parameters of the sprayer chassis and the tank

Parameters/Units	Value
m_s / kg	620
m_{tl} , m_{tr} / kg	70
I_{xx} / kgm^2	600
k_{sl} , k_{sr} / N/m	27350
c_{sl} , c_{sr} / Ns/m	985
k_{tl} , k_{tr} / N/m	309500
h_T / m	0.3
B / m	1.6
l_f / m	1.3
w_f / m	1.1

Note: h_f depends on the liquid filling ratio, given in the following paragraph

Apart from these parameters mentioned above, there are some parameters that are constantly changing during pesticide application. The liquid in the tank is continuously consumed during the application process, so its mass and moment of inertia change continuously. In addition, the driving speed of the sprayer will also change constantly in order to adapt to different working conditions. Obviously, the vertical acceleration acting on the tire is different when the sprayer passes over the same ground at different speeds. Undoubtedly, these factors will affect the roll stability of the sprayer. Therefore, the liquid filling ratio and the driving speed of the sprayer are used as the variable parameters in the simulations.

When there is little liquid in the tank, the sloshing force will not be large even if all the liquid is involved in the shaking. On the other hand, if the tank is filled with the liquid, the sloshing force is also reduced to some extent because the movement of the liquid is restricted by the top cover of the tank. Therefore, the maximum sloshing force generally occurs at medium liquid depths (*Zheng et al., 2020*). The amount of liquid can be defined by the filling ratio, that is, the ratio of the liquid volume to the tank capacity. Therefore, the filling ratio is chosen to be 0.3, 0.6 and 0.9. The case of no liquid is also included in order to analyze the influence of liquid, that is, the filling ratio is 0. The capacity of the tank is 1000 L. The liquid is tap water.

To improve efficiency, sprayers need to travel at higher speeds when applying pesticides. However, the sprayer often needs to be operated at relatively low speeds when turning around at the end of the field or shifting the operation workplace. Taking all situations into account, four driving speeds are selected in the simulations, that is, 0.5 m/s, 1.0 m/s, 1.5 m/s and 2.0 m/s.

UNEVEN GROUND EXCITATION

There are inevitably some bumps or pits and other obstacles on the farmland and field road. Compared with hardened pavement in the urban, the ground of farmland is relatively rough, which is equivalent to E-level or F-level road. Even on relatively soft paddy fields, the roughness of the hard bottom is between D-level and

E-level (*Zhu et al., 2016*). When the wheels pass these obstacles during the pesticide application process of the sprayer, the liquid in the tank is prone to sloshing greatly.

The distribution of obstacles is unpredictable and the bumps and dips also appear randomly. Therefore, the spatial distribution of road surface roughness is random. In other words, the roughness of the road surface is different for different plots.

Therefore, the description of road surface roughness is based on statistical theory. Pavement roughness can be simulated using filtered white noise or sinusoid superposition method (*Xu, 2007*).

Here, the sinusoid superposition method is adopted to get the excitation of uneven ground.

The stochastic road spectrum can be written as:

$$q(x)=\sum_{i=1}^{m}\sqrt{2G_q\left(n_{mid,i}\right)\Delta n_i}\,\sin\left(2\pi n_{mid,i}x+\theta_i\right) \tag{12}$$

Where, $G_q(n)=G_q(n_0)\left(\frac{n}{n_0}\right)^{-w}$ is the fitting expression of the power spectrum density, [m^3]; n is the spatial frequency, [m^{-1}]; n_0 is the spatial frequency reference value, generally $n_0=0.1\mathrm{m}^{-1}$; Δn_i is the increment of the spatial frequency, [m^{-1}]; $n_{mid,i}$ is the central frequency of the *i*-th spatial frequency, [m^{-1}]; x is the longitudinal position along the road, [m]; θ_i is the random numbers in range of $[0,2\pi]$; w is the frequency index, generally $w=2$. The typical stochastic spectrum of E-level road is shown in Fig.4.

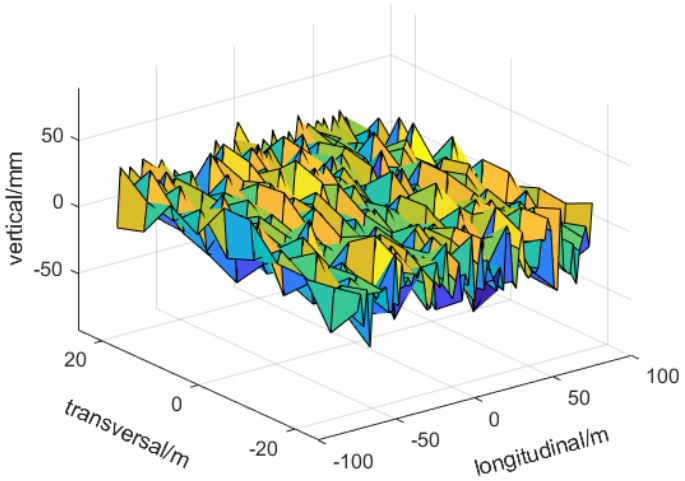

Fig. 4 - Typical E-level 3D pavement

As mentioned earlier, the roll stability of the sprayer under the liquid sloshing force is the main objective in this article. Therefore, the two-dimensional distribution of the uneven pavement is enough to describe the excitations generated from the ground. That is, the sprayer drives in the longitudinal direction and the unevenness along the vertical direction acts on the left and right wheel. Taking the driving speed into account, the spatial distribution of the uneven ground can be converted into the excitation that changes with the time. Obviously, the excitations acting on the wheels are also random, as shown in Fig. 5.

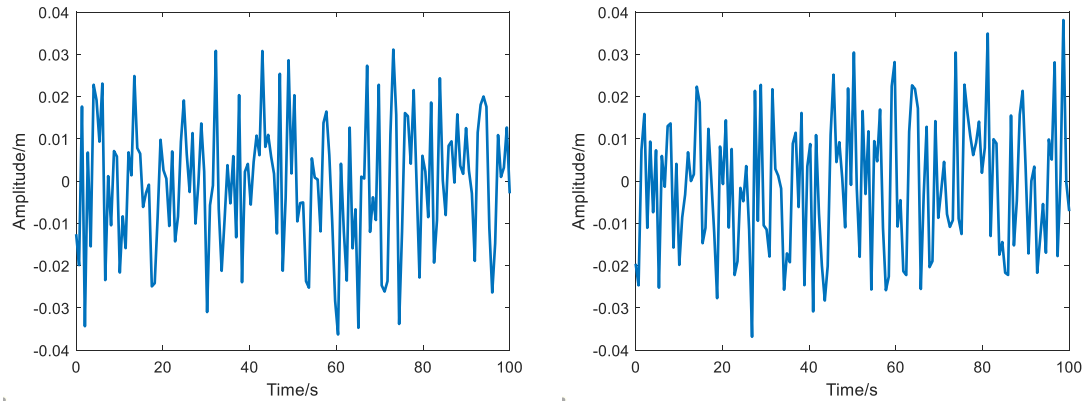

Fig. 5 - Typical excitation on left and right wheel

RESULTS

EFFECT ON ROLL ANGLE

The roll angle of the frame can distinctly reflect the roll of the sprayer. The change of the roll angle with time at different filling ratio and speeds is shown in Fig. 6, where, v is the driving velocity and the numbers in the legend are filling ratio.

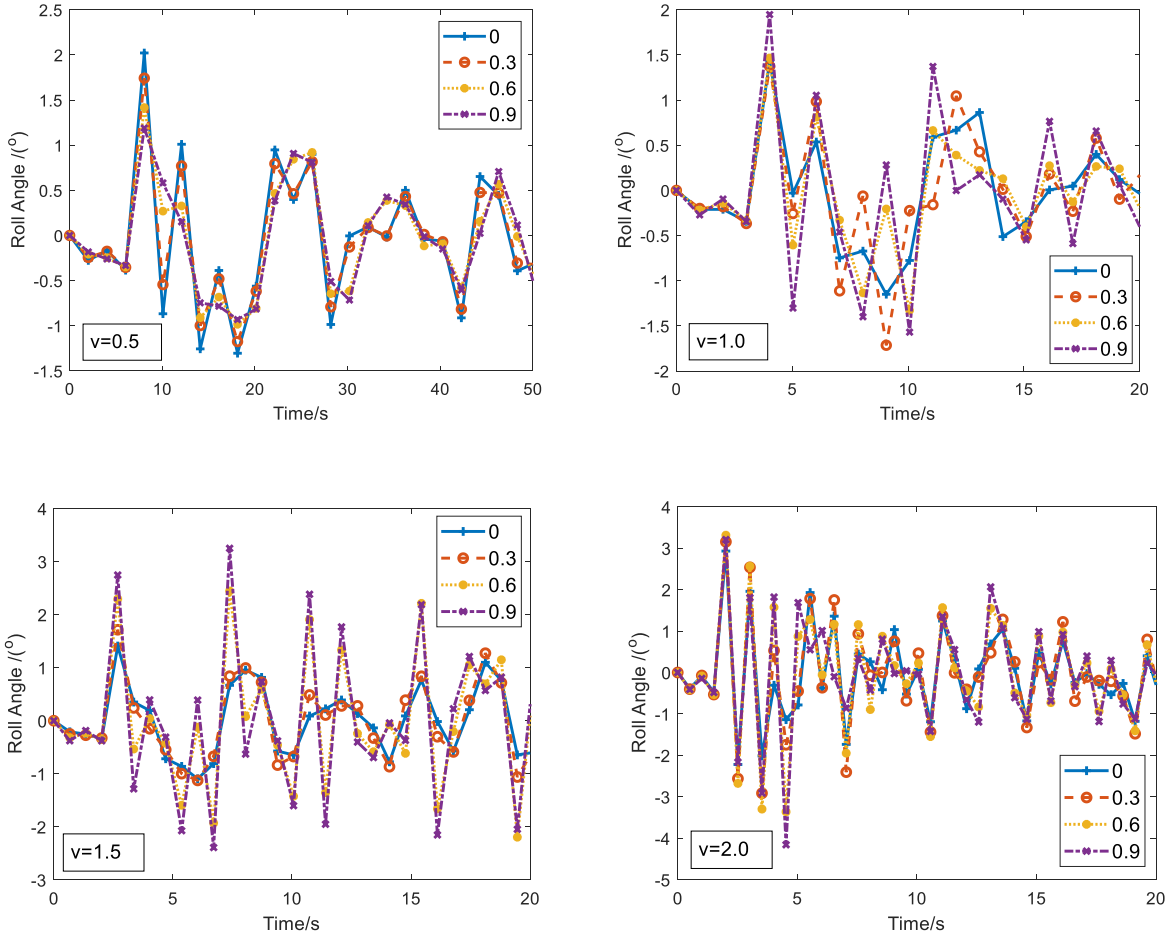

Fig. 6 - Roll angle of the sprayer at different filling ratios and driving speeds

It can be seen that the influence of filling ratio on the roll angle is different for a different driving speed. When the speed is low (v=0.5 m/s), the roll angle in the presence of liquid is smaller than that in the absence of liquid, and the roll angle decreases as the filling ratio increases; with the increase of velocity (v=1.0 m/s and v=1.5 m/s), the roll angle in the presence of liquid is larger than that in the absence of liquid, and the larger the liquid filling ratio, the larger the roll angle. When the speed increases to v=2 m/s, the shape of the roll angle

curves corresponding to different filling ratios is a little different. However, in general, the roll angle of the vehicle body with the liquid is greater than that without liquid.

The reasons are interpreted as follows. The tire displacement is basically consistent with the terrain change when sprayers drive at low speed. In this case, the vehicle body faces rolls, but the angular velocity is small. Therefore, the movement of the liquid in the horizontal direction is not violent. The impact effect of the liquid on the tank wall is not significant, and it is mainly manifested as a change in the position of the centroid of the liquid. Considering that the liquid sloshing has a certain degree of lag relative to the displacement of the vehicle body, the change of the position of the liquid centroid reduces the inclination of the body instead. The larger the liquid filling ratio, the larger the change in the position of the centroid of the liquid. So, the offset effect of the liquid on the roll angle is more obvious. However, when the sprayer passes over ground at a higher speed, the roll angular velocity of the vehicle body becomes larger, and the excitation on the liquid also increases. The liquid is prone to sloshing greatly under large amplitude and high frequency excitations and produces a significantly increased sloshing force on the tank wall. In addition, the larger the liquid filling ratio, the larger the liquid sloshing force. So, the roll angle increases with the increase of the filling ratio.

It can also be seen that the roll angle generally increases as the speed increases. However, the maximum roll angle does not change much under the case of absence of liquid. In other words, the increase of the roll angle is mainly due to the contribution of the liquid. The reason may be the sloshing force formed by the reciprocating oscillation of the liquid under the excitation of uneven ground. Higher velocities mean more violent oscillations and thus greater horizontal sloshing forces act on the vehicle frame. Therefore, the vehicle body is more likely to roll when the sprayer passes over the uneven ground at higher speeds.

EFFECT ON FRAME ACCELARATION

The motion of the vehicle frame also includes vertical vibrations in addition to roll. The frame vibration also affects the pressure of the tires on the ground through the transmission of the suspension. This pressure is also an important indicator of roll stability. The vertical acceleration of the sprayer frame at different filling ratio and speeds is shown in Fig. 7.

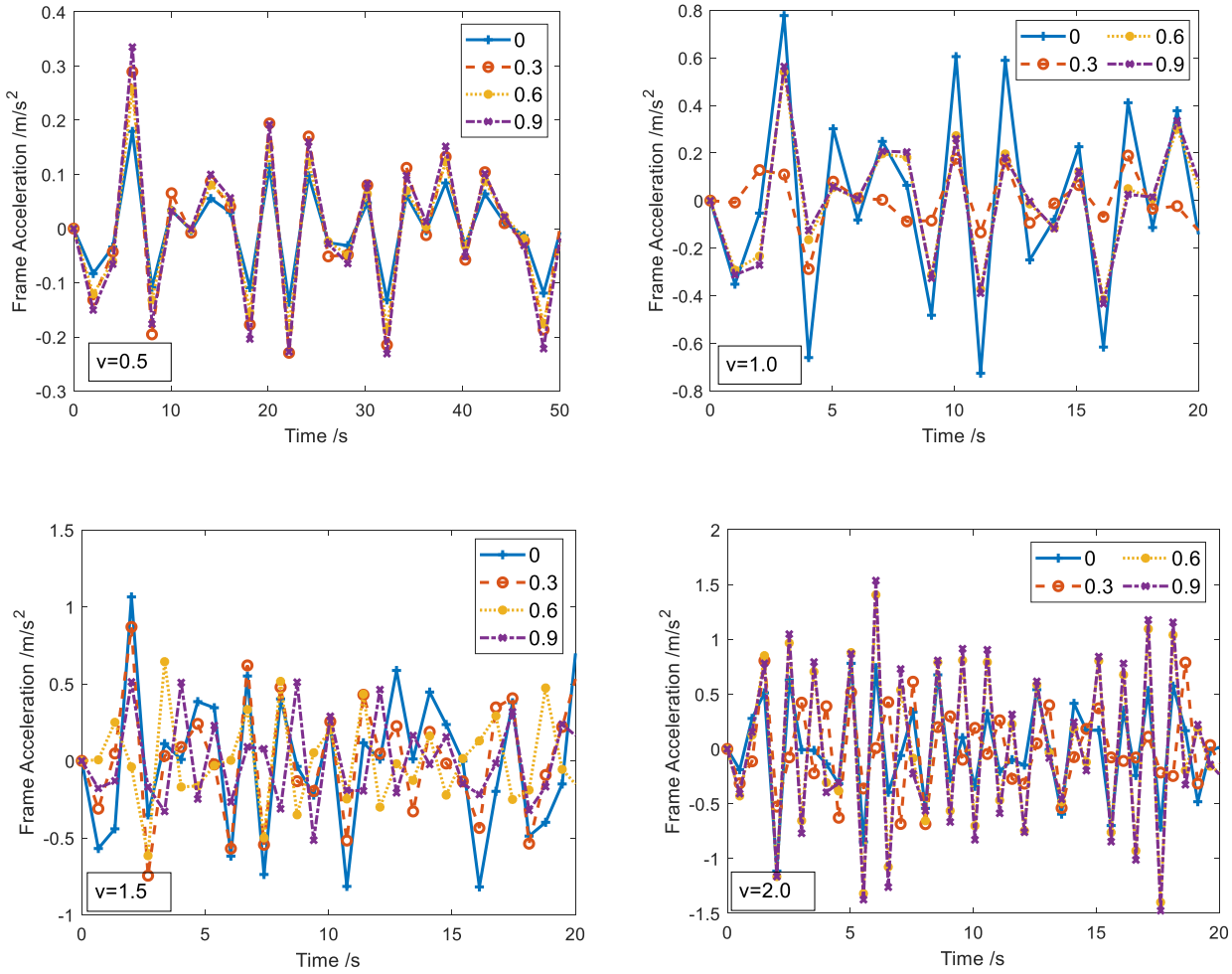

Fig. 7 - Frame acceleration of the sprayer at different filling ratio and driving speed

When the speed is low or high ($v = 0.5\text{m/s}$, $v = 2.0\text{m/s}$), the vertical acceleration of the vehicle body in the presence of liquid is greater than that in the absence of liquid, and the acceleration increases with the increase of the filling ratio. However, when the speed is medium, the acceleration of the vehicle frame in the presence of liquid is less than that in the absence of liquid. The acceleration is the smallest when the filling ratio is 0.3 for $v = 1.0\text{m/s}$, while in the case of $v = 1.5\text{m/s}$, the larger the filling ratio the smaller the acceleration.

The reason may lie in the combined action of the liquid sloshing force and gravity. When the speed is low, the liquid sloshing force is small and the effect of the mass of the liquid on the vertical acceleration is more significant. The increase of the acceleration is mainly due to the presence of the liquid gravity. On the other hand, a larger liquid mass corresponds to a larger inertial force. Therefore, the vertical acceleration of the frame is attenuated by this force when the sprayer drives at medium speed because the effect of the horizontal sloshing force is relatively weak.

However, the sloshing force will increase significantly if the sprayer passes over uneven ground at high speed. The influence of sloshing force is more important under this situation. So, the acceleration increases with the increase of filling ratio again.

In addition, it can be seen that the vertical acceleration increases generally as the speed increases. Similarly, the presence of liquid plays an important role in the increase of the acceleration. Therefore, the presence or absence of the liquid has significant effect on the roll stability of the sprayer that is subjected to the excitation from the uneven ground.

CONCLUSIONS

Based on the equivalent mechanical model of liquid sloshing and related experimental results, considering the vertical and roll motion of the vehicle body and the sloshing of the liquid in the tank, a coupling dynamic model of the sprayer was established. The roll stability of the sprayer under the excitation of uneven ground was studied, and the effects of the liquid filling ratio and driving speed on the roll angle and the vertical acceleration of the vehicle frame were analyzed. The results show that:

(1) The effect of the liquid filling ratio is related to the driving speed. The roll angle decreases with the increase of filling ratio at low speed, but it increases with the increase of the filling ratio at high speed. However, the changes of the vehicle frame acceleration with the liquid filling ratio are almost opposite.

(2) In general, both the roll angle and the vertical acceleration of the sprayer frame increase with the increase of the driving speed, especially with the presence of liquid. Therefore, the influence of liquid sloshing on roll stability cannot be ignored for sprayers that often travel on uneven ground.

ACKNOWLEDGEMENT

This work was financially supported by the Key Laboratory of Modern Agricultural Equipment, Ministry of Agriculture and Rural Affairs, P. R. China (grant no. HT20160351), the China Agriculture Research System of MOF and MARA (Grant No. CARS-12) and the Agricultural Science and Technology Innovation Project of the Chinese Academy of Agricultural Sciences, Crop Protection Machinery Team (Grant No. CAAS-ASTIP-CPMT).

REFERENCES

[1] Abramson H. N. (1966). *The dynamic behavior of liquids in moving containers*. NASA SP-106, Washington / USA

[2] Chen Yu, Mao Enrong, Li Wei et al. (2020). Design and experiment of a high-clearance self-propelled sprayer chassis, *International Journal of Agricultural and Biological Engineering*, Vol.13, pp. 71-80, Beijing / China

[3] Cui Longfei, Mao Hanping, Xue Xinyu et al. (2018). Optimized design and test for a pendulum suspension of the crop spray boom in dynamic conditions based on a six DOF motion simulator, *International Journal of Agricultural and Biological Engineering*, Vol. 11, pp. 76-85, Beijing / China

[4] Deng Mingle, Yue Baozeng, Huang Hua. (2016). Study on the Equivalent Mechanical Model for Large Amplitude Slosh(液体大幅晃动类等效力学模型研究), *Journal of Astronautics*, Vol. 37, pp. 631-638, Beijing / China

[5] Ding Kai, Feng Jing'an, Wang Weibing, et al. (2019). Scale model experiment of stability for high-clearance sprayer affected by multi-factors (多因素影响下高地隙喷雾机稳定性模型试验), *Journal of Jiangsu University (Natural Science Edition)*, Vol. 40, pp. 538-546, Jiangsu / China

[6] Hu Xiaoming, Li Wanli, Sun Li et al. (2013). Liquid sloshing reduces driving stability of semi-trailer liquid tank (液体晃动降低半挂液罐车行驶稳定性), *Transactions of the Chinese Society of Agricultural Engineering*, Vol. 29, pp. 49-58, Beijing / China

[7] Ibrahim R. A. (2005). *Liquid Sloshing Dynamics*, Cambridge University Press, Cambridge/UK

[8] Li Qing, Ma Xingrui, Wang Tianshu. (2011). Equivalent Mechanical Model for Liquid Sloshing in Non-Axisymmetric Tanks (非轴对称贮箱液体晃动的等效力学模型), *Journal of Astronautics*, Vol. 32, pp. 242-249, Beijing / China

[9] Pochi D., Vannucci D. (2002). A System with Potentiometric Transducers to Record Spray Boom Movements under Operating Conditions, *Biosystems Engineering*, Vol. 82, pp. 393-406, San Diego/USA

[10] Qiu Wei, Li Xiaolong, Li Chongchong, et al. (2020). Design and test of a novel crawler-type multi-channel air-assisted orchard sprayer, *International Journal of Agricultural and Biological Engineering*, Vol. 13, pp. 60-67, Beijing/China

[11] Tahmasebi M, Rahman R A, Mailah M, et al. (2015). Roll movement control of a spray boom structure using active force control with artificial neural network strategy, *Journal of Low Frequency Noise Vibration & Active Control*, Vol. 32, pp. 189-202, Brentwood/UK

[12] Wu Xiuheng, Qin Jiahao, Du Yuefeng, et al. (2018). Experiments of vibration control for active pneumatic suspension system in high clearance self-propelled sprayer (高地隙喷雾机主动空气悬架减振控制与实验), *Transactions of the Chinese Society for Agricultural Machinery*, Vol. 49, pp. 60-67, Beijing/China

[13] Xu Yanhai. (2007). Computer simulation on stochastic road irregularities (随机路面谱的计算机模拟), *Transactions of the Chinese Society for Agricultural Machinery*, Vol. 38, pp. 33-36, Beijing/China

[14] Xue Tao, Li Wei, Du Yuefeng, et al. (2018). Adaptive fuzzy sliding mode control of spray boom active suspension for large high clearance sprayer (大型高地隙喷雾机喷杆主动悬架自适应模糊滑模控制), *Transactions of the Chinese Society of Agricultural Engineering*, Vol. 34, pp. 47-56, Beijing/China

[15] Yang Fangfei, Han Xiaojin, Duan Yaoqi et al. (2014). Reliability experiment on high clearance boom sprayer chassis (高地隙喷杆喷雾机底盘可靠性试验), *Transactions of the Chinese Society for Agricultural Machinery*, Vol. 45, pp. 73-77, Beijing/China

[16] Yu Xisheng, Feng Jing'an, Wang Qigan, et al. (2020). Study on active torque controller for roll stability of high clearance vehicles (高地隙车辆侧倾稳定性主动力矩控制器的研究), *Journal of Jiangsu University (Natural Science Edition)*, Vol. 4, pp. 8-14, Jiangsu/China

[17] Zeng Shan, Liu Jun, Luo Xiwen et al. (2019). Design and experiment of wheel-track compound power chassis for high clearance sprayer in paddy field (水田高地隙喷雾机轮履复合动力底盘的设计与试验), *Journal of South China Agricultural University*, Vol. 40, pp. 14-22, Guangzhou/China

[18] Zhai Changyuan, Landers Andrew, Zhang Bo. (2018). An RFID-based solution for monitoring sprayer movement in an orchard/vineyard, *Precision Agriculture*, Vol. 19, pp. 477-496, Dordrecht/Netherlands

[19] Zheng Jizhou, Han Xiang, Guo Haoran, et al. (2020). Experimental study of liquid sloshing force characteristics in rectangular tank of sprayer under harmonic excitation, *INMATEH-Agricultural Engineering*, Vol. 62, pp. 125-132, Bucharest/Romania

[20] Zheng Xuelian, Li Xiansheng, Ren Yuanyuan et al. (2013). Equivalent mechanical model for liquid sloshing in partially-filled tank vehicle (非满载汽车罐车液体冲击等效机械模型), *Journal of Jilin University (Engineering and Technology Edition)*, Vol. 43, pp. 1488-1493, Changchun/China

[21] Zhou Qianqian, Wen Haojun, Li Zhongxiang, et al. (2020). Design and Test of Fuzzy Anti-skid Control of Four-wheel Drive Hydraulically Driven Sprayer(液压四驱喷雾机模糊防滑控制系统设计与试验), *Transactions of the Chinese Society for Agricultural Machinery*, Vol. 51, pp. 283-288, Beijing/China

[22] Zhu Sihong, Ma Jiafu, Yuan Jiaqi, et al. (2016). Vibration characteristics of tractor in condition of paddy operation (水田作业工况的拖拉机振动特性), *Transactions of the Chinese Society of Agricultural Engineering*, Vol. 32, pp. 31-38, Beijing/China